Centrifuge modelling on seismic response of layered clayey sand ground during earthquake swarms

W.J. Liu, L. Li, B. Zhu
College of Civil Engineering and Architecture, Zhejiang University, Hangzhou, China, vinzeel@zju.edu.cn, li_lu@zju.edu.cn, binzhu@zju.edu.cn

J.C. Li, D.Q. Kong
Center for Hypergravity Experimental and Interdisciplinary Research, Zhejiang University, Hangzhou, China, lijunchao@zju.edu.cn, deqiong_kong@zju.edu.cn

ABSTRACT: The frequent occurrence of major earthquake swarms worldwide has posed severe threats to geotechnical structures. This study investigates the dynamic response of layered clayey sand grounds subjected to earthquake swarm sequences through centrifuge model tests at 50g. Two models, with and without a surcharged block, are considered. The former model is designed to mimic the ground with large dam above it. Data acquisition primarily include quake-induced acceleration, excess pore pressure, and surface settlement. The mechanisms of soil dynamic behaviour and liquefaction potential under single strong-motion events and consecutive seismic events are analysed. The results demonstrate that the free ground liquefaction occurs alongside significant soil dilation. Consecutive strong motions induce continuous accumulation and escalation of excess pore pressure in the lower clayey layer. The surcharged block seems to exhibit suppressive effect on the excess pore pressure accumulation during shaking, and pore pressure dissipation after that. Notably, consecutive seismic events accelerate peak excess pore pressure generation in the foundation. These findings may help improve the seismic design of geotechnical structures in regions vulnerable to earthquake swarms.

1 INTRODUCTION

In recent years, the frequent occurrence of earthquake swarms worldwide has posed serious threats to geotechnical structures. These swarms, consisting of spatiotemporally clustered moderate to strong seismic events, can induce cumulative effects such as soil stiffness degradation and continuous buildup of excess pore water pressure. This significantly increases the liquefaction risk of dam foundations, posing a more severe threat to the seismic safety of major engineering structures like large dams.

In the field of seismic response and liquefaction mitigation for dam foundations, centrifuge shaking table testing is widely recognized as a reliable and effective method, as it accurately replicates the stress states of prototypes in scaled models (Han et al., 2016; Kutter et al., 2018). Previous studies using this technique have enhanced the understanding of seismic responses of dam-foundation systems (Sharp and Adalier, 2006; Kim et al., 2011) and the effectiveness of anti-liquefaction measures such as stone columns and sheet-pile walls (Cao et al., 2024; Liu et al., 2025). However, existing research has predominantly focused on the impact of single seismic events, leaving the cumulative response mechanisms of foundations subject to large dams under earthquake swarm sequences poorly understood.

To address this gap, this study conducts centrifuge shaking table tests on saturated dam foundations to systematically investigate the dynamic behaviour of layered clayey sand under earthquake swarm sequences. Two test conditions—with and without an overlying dam surcharge—are considered. By monitoring acceleration, excess pore water pressure, and surface settlement, the dynamic behaviour and liquefaction potential of the soil under both single strong motions and consecutive seismic events are analysed. The findings aim to provide theoretical and experimental support for the seismic design of dam foundations in regions prone to earthquake swarms.

2 EXPERIMENTAL SETUP

2.1 Model configurations

This study selected a prototype from a second-class large hydropower project located in southwestern China, with a maximum dam height of 38 m. The site predominantly consists of clayey sand and is situated in the seismically active Xianshuihe fault zone. To assess the seismic safety of the dam foundation, two centrifuge shaking table tests were conducted at 50g, investigating the dynamic response of the foundation, including a free-field foundation without a dam surcharge (Test-1) and a foundation with a dam surcharge (Test-2), as shown in Figure 1. The model design adhered to the general scaling laws of centrifuge modeling, with a length scale of $1/n$ (n=50), a stress scale of 1, and a dynamic time scale of $1/n$. To simultaneously satisfy the scaling requirements for dynamic and consolidation times, silicone oil with a viscosity 50 times that of water (ρ = 955 kg/m^3 at 25°C) was used as the pore fluid.

The tests were performed on the ZJU-400 geotechnical centrifuge at Zhejiang University, which has a payload capacity of 400 g·tons and an effective radius of 4.5 m. The centrifuge is equipped with a servo-hydraulic, unidirectional shaking table capable of achieving a maximum acceleration of 40g and a maximum displacement of 0.6 cm. A laminar shear model container with internal dimensions of 740 mm × 340 mm × 425 mm (length × width × height) was used. The container consists of 12 stacked aluminum frames that are designed as a low-stiffness laminar stack. This configuration imposes a tied lateral boundary condition, enabling the soil to undergo shear deformation freely during shaking and minimizing spurious wave reflections.

2.2 Materials and preparation

The foundation model had a height of 400 mm, representing a 20 m thick soil deposit in prototype scale. Based on the typical stratigraphy of a site in Southwest China, the foundation was simplified into a two-layer system: a 100 mm thick upper layer (5 m in prototype) and a 300 mm thick lower layer (15 m in prototype). The soils, classified as clayey sands, were retrieved from depths of 3.2 m and 10.5 m at the site. These soils were processed in the laboratory by crushing, oven-drying, and passing through a 2 mm sieve to obtain dry soil samples. Their physical properties are summarized in
Table 1.

Table 1. Physical properties of soils.

Soil	Upper layer	Lower layer
D_r	82%	64%
G_s	2.696	2.677
ρ_{max} (kg/m^3)	1659	1634
ρ_{min} (kg/m^3)	1178	1082
I_p	11.0	14.5
k (m/s)	4.93×10^{-6}	8.13×10^{-7}

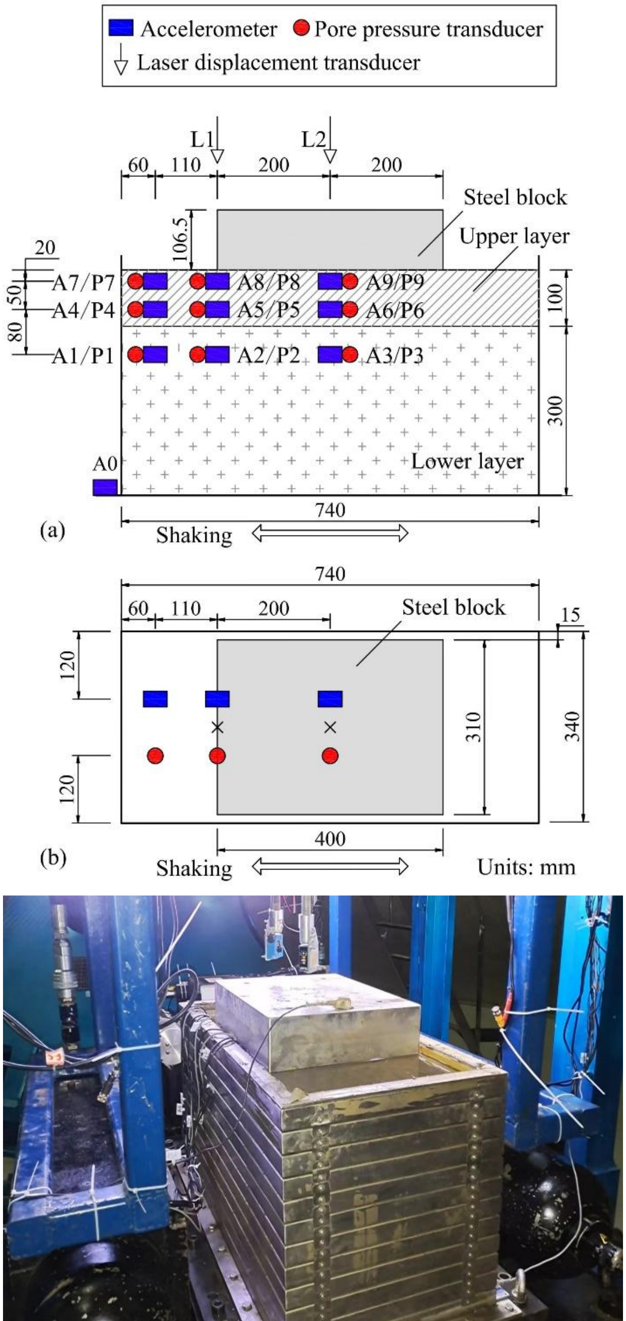

Figure 1. Model configuration of Test-2: (a)side view and (b) top view (model scale);(c) photogragh of the model.

Due to the significant fines content, the air-pluviation method was deemed unsuitable as it could lead to substantial particle segregation and loss. Therefore, the dry tamping method was employed for model construction. The dry soil was placed in layers and compacted to the target density, thus forming the dry soil model. Subsequently, the model was saturated by slowly permeating silicone oil under vacuum conditions, achieving the desired saturated soil foundation for testing.

To equivalently simulate the effect of contact pressure from the overlying dam on the dynamic response of the foundation, and to ensure that the stress distribution within the foundation soil in the model matched that of the engineering prototype, the foundation contact stress of the prototype gate dam was computed using Geostudio software. Based on the computed results, a rectangular steel block measuring 400 mm × 310 mm × 106.5 mm (length × width × height) was selected and placed atop the foundation model to simulate the surcharge load imposed by the prototype dam. The steel block applies a vertical stress of approximately 375.3 kPa under the dam centreline and 1189.7 kPa under the dam edge at the foundation surface, corresponding to the prototype dam's contact pressure (Liu et al., 2025).

2.3 Input motions and data acquisition

After a 9.5-hour consolidation under a 50*g* centrifugal acceleration (approximately 20 days in prototype scale), a sequence of seismic motions was applied to the models. The input motion was based on a real earthquake record from Southwest China, scaled to a peak horizontal acceleration of 0.3*g*. To simulate the characteristics of earthquake swarms, the input sequence consisted of a mainshock event followed by two successive aftershock events. The testing protocol involved first applying a single 0.3*g* mainshock (Sequence M1). After the excess pore pressures in the foundation had sufficiently dissipated, two consecutive 0.3*g* aftershocks (Sequences M2 and M3) were applied. The triggering time of M3 was not fixed, instead, it manually triggered when the excess pore pressure at mid-depth sensors had dissipated to approximately half of the peak value recorded during M2. The test program, summarized in Table 2, was designed to investigate the cumulative damage effects on the dam foundation under successive seismic events.

Table 2. Test arrangement.

Model	Test No.	Motion
Free field	Test-1-M1	0.3*g* single mainshock
	Test-1-M2 Test-1-M3	0.3*g* consecutive aftershocks
Foundation with a dam surcharge	Test-2-M1	0.3*g* single mainshock
	Test-2-M2 Test-2-M3	0.3*g* consecutive aftershocks

In Test-2 (foundation with a dam surcharge), pore pressure transducers (P1–P9) and uniaxial accelerometers (A1–A9) were installed to measure the pore pressure and acceleration responses representing different stress state: soil with negligible influence from the surcharge, under the edge of the surcharge wherelarge static shear stress exists, and right under the center of the surcharge where large effective confining stress exists. Two laser displacement transducers (L1, L2) were used to record surface settlement, and a triaxial accelerometer (A0) monitored the input motion at the shaking table. The same sensor arrangement was implemented in Test-1 (free field) at corresponding locations for comparative analysis. As the seismic response was primarily concentrated in the upper foundation layer, monitoring efforts focused on this zone. Consequently, two vertical arrays of sensors were installed within the upper soil layer, with one array placed in the lower layer, as illustrated in Figure 1.

3 TEST RESULTS

Through two series of shaking table centrifuge model tests (Test-1 and Test-2), the dynamic responses of acceleration and pore pressure at various locations within the ground were systematically examined. All experimental results presented in this paper have been converted to prototype scale according to a centrifugal acceleration of 50*g*.

3.1 Acceleration responses

The input acceleration recorded at A0 was identical for Test-1 and Test-2, ensuring a consistent base excitation. Figure 2 illustrates the acceleration time histories recorded in Test-1 and Test-2 during a single mainshock event (M1). In the lower layer (A1–A3), the acceleration responses of the two models were broadly comparable. Seismic motions propagated upward from the base with limited attenuation, and the input motion largely preserved its original frequency content, indicating that the deeper soil layer remained relatively stiff and did not undergo significant nonlinear degradation during shaking. However, distinct differences emerged as seismic motions propagated through the upper layer. In the free field (Test-1), acceleration amplitudes progressively increased with elevation. At A7–A9, the acceleration records displayed multiple sharp peaks between 10 s and 14 s. These transient spikes are indicative of pronounced soil dilation in the dense clayey sand during cyclic shearing, which temporarily increased shear stiffness and enhanced high-frequency motion transmission (Olarte et al., 2017; Cao et al., 2023). Subsequently, a marked reduction in acceleration amplitude occurred at approximately 15 s, producing a clear "shrinking" phenomenon in the time histories. This response suggests substantial soil softening, likely associated with the rapid buildup of excess pore pressure, which impeded shear wave propagation and reduced effective stress. Following this softening stage, partial dissipation of excess pore pressure allowed a gradual recovery of foundation stiffness. Following that, acceleration amplitudes increased again, accompanied by a noticeable elongation of the dominant response period. In contrast, no comparable softening or dilation behaviour was observed in the lower clayey layer.

Compared with the free field, the presence of a rigid surcharged block in Test-2 significantly altered the seismic response of the upper foundation. The surcharge imposed a rigid boundary constraint that inhibited the upward propagation and amplification of seismic waves, particularly beneath the edge of the surcharged at the foundation surface (A8). Notably, the acceleration time history at A8 exhibited an absence of positive acceleration peaks during shaking. This asymmetric response is likely attributable to the elevated initial static shear stress induced by the overlying load (Maharjan & Takahashi, 2014).

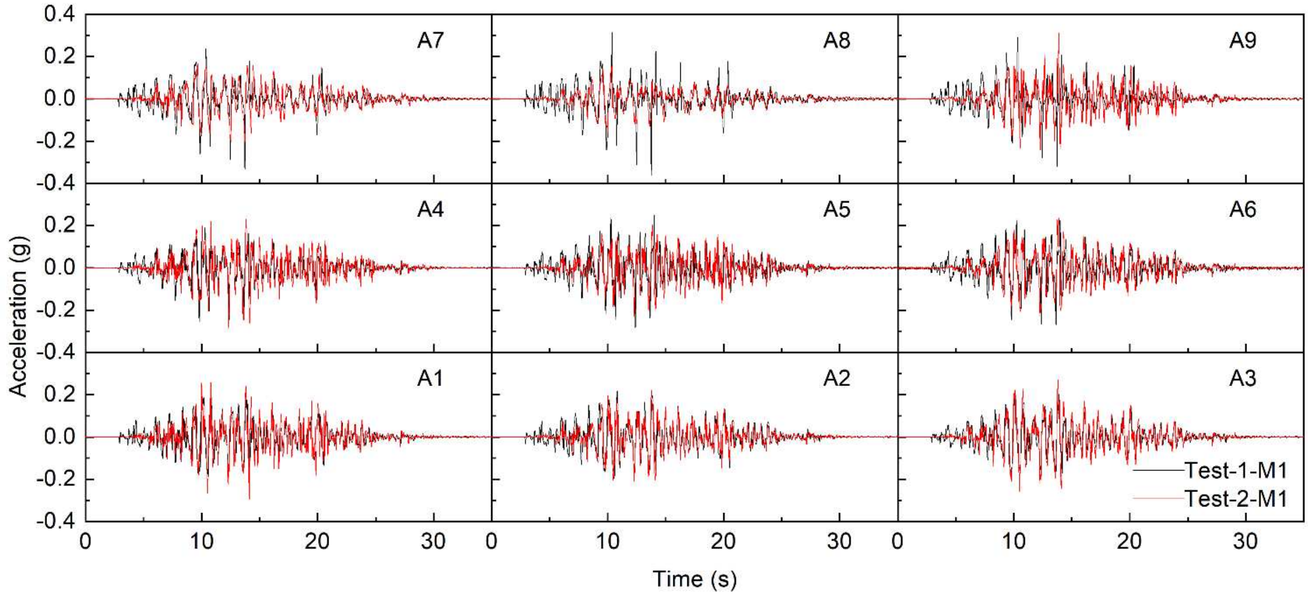

Figure 2. Time histories of acceleration in Test-1 and Test-2 under M1.

Figure 3 presents the depth-wise distribution of the peak acceleration amplification factor for the free field in Test-1 and for the foundation directly beneath the surcharged in Test-2. The amplification factor is defined as the ratio between the peak acceleration recorded at a given location and that measured at the shaking table (A0). In the lower layer, characterised by a higher fine-grained content, peak accelerations in both models exhibited a gradual attenuation with decreasing depth. This behaviour suggests that the lower clayey sand layer acted as an energy-dissipative medium during seismic wave propagation. Within this layer, the peak accelerations beneath the surcharged were consistently higher than those observed in the free field. Nevertheless, the aftershocks futher led to a progressive reduction in peak acceleration in the surcharged foundation. In the upper layer, contrasting trends were observed. In Test-1, peak accelerations increased progressively towards the ground surface, reaching a maximum at the shallowest measurement point. Continuous seismic shaking further amplified this trend. Examination of the corresponding acceleration time histories indicates that the elevated peak values were associated with pronounced sharp spikes, reflecting transient stiffness increases caused by soil dilation. This observation implies that consecutive seismic events intensified the dilative response of the dense clayey sand, thereby enhancing acceleration amplification during upward wave propagation. In contrast, the variation of peak acceleration in the surcharged foundation was more complex. Although local amplification occurred at certain depths, the overall peak accelerations at the uppermost measurement points showed a successive decrease with repeated shaking. This response highlights the combined effects of surcharge-induced confinement, suppression of soil dilation, and cumulative plastic deformation under earthquake swarm loading. The results demonstrate that the surcharged block fundamentally altered the acceleration amplification mechanism in the upper foundation, particularly during consecutive seismic events.

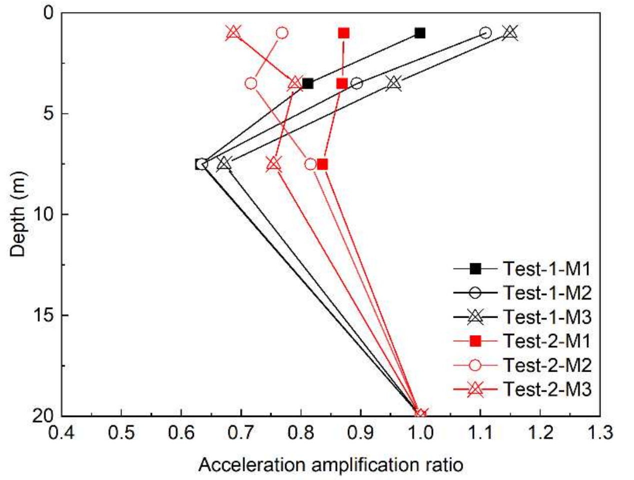

Figure 3. Acceleration amplification ratio in Test-1 and Test-2 under M1, M2 and M3.

3.2 Pore pressure responses

Figure 4 shows the time histories of the excess pore pressure ratio for both foundation models under seismic loading. The excess pore pressure ratio, defined as $r_u = \Delta u/\sigma'$ (where Δu is the excess pore pressure and σ' is the initial effective stress), is a key indicator for assessing soil softening and liquefaction potential in cohesionless and low-cohesion soils. While loose sands typically reach $r_u \approx 1.0$ at liquefaction, soils with higher fines content often experience incomplete liquefaction, with r_u values commonly ranging between 0.90 and 0.95 during severe softening (Ishihara, 1993). In this study, for the computation of r_u in Test-2, the additional vertical stress imposed by the block was accounted for. Under the single mainshock event M1, r_u at P8 (depth = 1 m) and P5 (depth = 3.5 m) in the free field rapidly exceeded 0.9, indicating a near-liquefied state in the upper layer. In contrast, r_u in the lower layer remained around 0.5, reflecting limited pore pressure accumulation due to higher fines content and lower cyclic mobility. Owing to the relatively low permeability of the clayey sand, post-shaking pore pressure dissipation was slow, allowing elevated pore pressures to persist between seismic events.

In the surcharged foundation, r_u development showed pronounced spatial variability. Outside the surcharged zone, where the additional vertical stress was relatively small, r_u increased to approximately 0.8–0.9. Beneath the edge of the surcharge, pore pressure generation was significantly inhibited, while directly beneath the surcharge, the higher confining pressure limited r_u to around 0.6. These results indicate that although the surcharge effectively reduced the liquefaction potential beneath the loaded area, a non-negligible risk of seismic softening or liquefaction persisted in the peripheral zones.

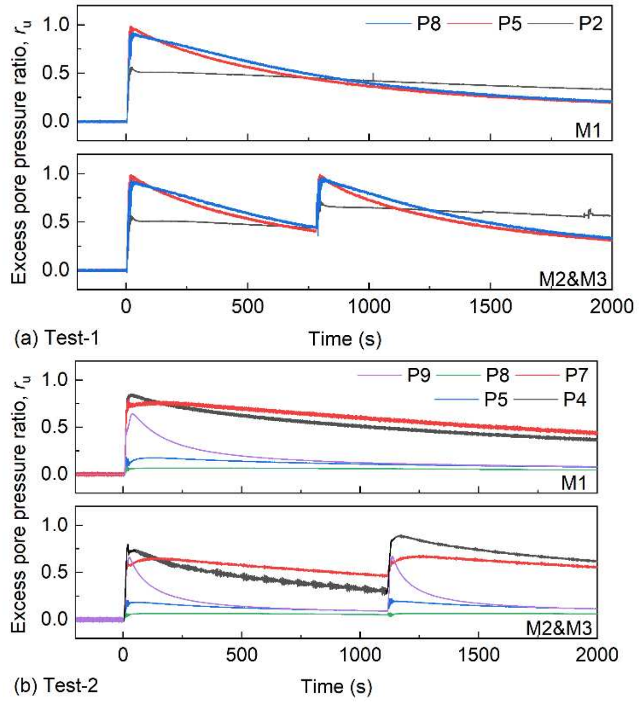

Figure 4. Time histories of excess pore pressure ratio (r_u) in (a) Test-1 and (b) Test-2 under M1, M2 and M3.

Figure 5 presents the maximum excess pore pressure ratio ($r_{u,max}$) during the three seismic motions. In the shallow free field, where the soil had already reached a near-liquefied state after M1, the aftershocks (M2 and M3) had only a limited influence on $r_{u,max}$. In contrast, in the deeper free field layer, $r_{u,max}$ remained nearly unchanged during M2 but increased by approximately 30% during the immediately following M3, highlighting the delayed accumulation effect associated with consecutive seismic loading. In the surcharged foundation, $r_{u,max}$ beneath the surcharge and the surcharge edge was only marginally affected by aftershocks, with slight increases observed at P9 and P5 during M2 and M3. Outside the surcharged zone (P7 and P4), partial pore pressure dissipation and soil densification after M1 resulted in a noticeable reduction in $r_{u,max}$ during M2. However, M3 triggered renewed pore pressure accumulation, indicating that the beneficial effects of densification can be overridden by closely spaced seismic events. Notably, at P4—where $r_{u,max}$ was initially the highest in the model—the liquefaction risk increased further after the full sequence of motions. Overall, these results suggest that if excess pore pressures dissipate completely after a single mainshock, aftershaock may lead to similar or reduced $r_{u,max}$ owing to soil densification. However, under earthquake swarm conditions, incomplete dissipation often results in renewed and accelerated pore pressure accumulation, particularly in zones with poor drainage. Critical locations include P2 in Test-1, characterised by inherently low permeability, and the vicinity of P4 in Test-2, where steep pore pressure gradients retarded dissipation. This interpretation is supported by the time histories in Figure 4, which show a brief post-shaking rise in pore pressure at P7 and P4.

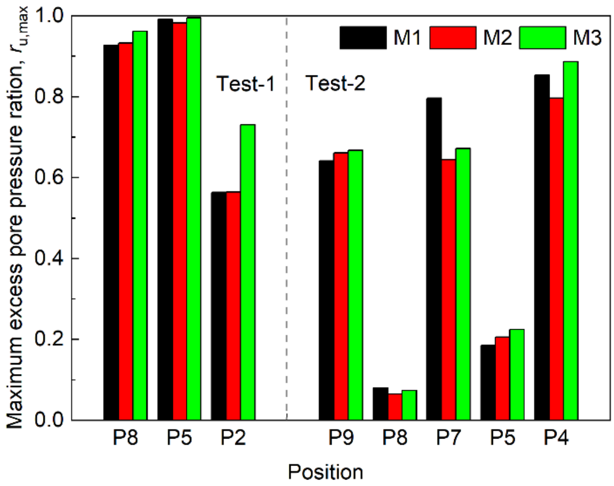

Figure 5. Maximum excess pore pressure ratio ($r_{u,max}$) in Test-1 and Test-2 under M1, M2 and M3.

3.3 Displacement responses

Figure 6 presents the detailed time histories of r_u in shallow layers and surface displacement during the three seismic motions, with surface displacement obtained from the average settlement measured at L1 and L2. The displacement data is expressed as normal strain in the vertical direction (ε_v), which is ratio of the surface vertical displacement and the thickness of the whole layers (Ghazy et al., 2025). Significant settlement initiated at approximately 10 s during all motions, as marked by the vertical dashed line. As seismic loading progressed, the rate of settlement gradually diminished and eventually stabilised. In the free field, the foundation underwent a final normal strain of 0.365% following a single mainshock, increasing to 0.735% after two consecutive aftershocks. The surcharged foundation experienced a normal strain of 0.68% after a single mainshock—approximately 1.9 times that of the free field—and 1.34% after consecutive aftershocks, corresponding to about 1.8 times the free field settlement. Moreover, the differential settlement between L1 and L2 provides an estimate of potential tilting of the surcharge block. After M1, the normal strain difference was only 0.005%, indicating negligible tilt. This difference increased to 0.015% after M2, and further to 0.065% after M3, suggesting that noticeable tilting developed as the seismic sequence progressed. While the initial asymmetry may partly reflect inherent ground heterogeneity, the progressive amplification of differential settlement under consecutive events—particularly when excess pore pressures had not fully dissipated—indicates that aftershocks can exacerbate non-uniform deformation, increasing the risk of instability for heavy surcharge structures.

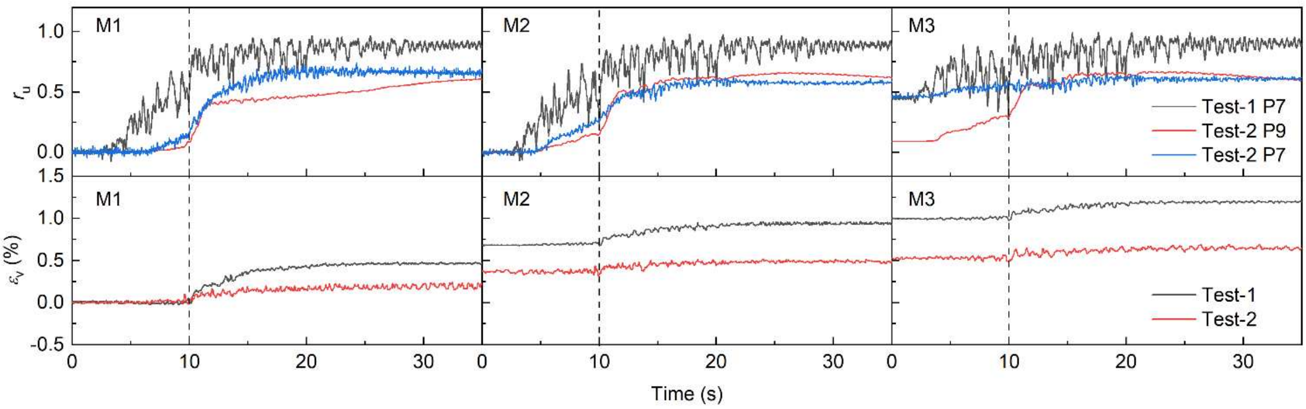

Figure 6. Time histories of excess pore pressure ratio (r_u) in shallow layers and normal strain (ε_v) under M1, M2 and M3.

In the free field, a distinct oscillatory drop in pore pressure occurred around 10 s, coinciding with the sharp acceleration spikes discussed earlier. This behaviour indicates pronounced soil dilation, which was particularly evident during M3. Following this stage, pore pressure remained close to its peak value with continued fluctuations, signalling the development of cyclic mobility. Substantial surface settlement accumulated subsequently as the soil underwent large irreversible strains. In the surcharged foundation, the excess pore pressure at P9 (right beneath the load) exhibited a clear acceleration in growth around 10 s during all three motions, reflecting a predominantly contractive soil response under high confining stress. At P7, located outside the surcharge, a similar accelerating trend was observed only during

M1 and was absent during M2 and M3. From this point onward, plastic deformation accumulated progressively beneath the surcharge, resulting in significant surface settlement. These observations demonstrate that consecutive seismic events can fundamentally alter the displacement mechanism of layered clayey sand foundations. While free field soils tend to exhibit dilative behaviour followed by cyclic mobility, surcharged foundations respond in a more contractive manner, with cumulative plastic deformation dominating settlement development. This distinction is particularly relevant for the seismic performance assessment of large geotechnical structures subjected to earthquake swarms.

4 CONCLUSIONS

This study investigated the seismic response of layered clayey sand ground subjected to earthquake swarm loading through 50*g* centrifuge model tests, considering both free field and surcharged foundation. The results demonstrate that soil stratification and surface surcharge exert significant control over acceleration amplification, excess pore pressure accumulation, and deformation mechanisms during consecutive seismic events. In the free field, upward propagation of seismic waves led to progressive acceleration amplification in the upper layer, accompanied by pronounced soil dilation, sharp acceleration spikes, and the development of cyclic mobility. Consecutive strong motions promoted cumulative excess pore pressure buildup, particularly in deeper layers with low permeability, thereby increasing liquefaction susceptibility even when the initial event did not cause full liquefaction.

The presence of a surcharge fundamentally altered the dynamic response of the foundation. The surcharge suppressed acceleration amplification and soil dilation beneath the load by increasing confining stress, effectively reducing liquefaction potential directly below the structure. However, this beneficial effect was spatially limited, as elevated pore pressure accumulation and renewed liquefaction risk were observed in peripheral zones outside the surcharge during consecutive aftershocks. Settlement responses further revealed that earthquake swarms significantly accelerated cumulative deformation, with surcharged foundations experiencing substantially larger and progressively tilting settlements than free field ground. Overall, the findings highlight that incomplete pore pressure dissipation between seismic events plays a critical role in amplifying damage during earthquake swarms, underscoring the need to explicitly account for cumulative effects in the seismic design of geotechnical structures founded on layered clayey sand.

ACKNOWLEDGEMENTS

The authors express their sincere gratitude toward the financial support from the National Natural Science Foundation of China (grant No.52588202) and the fund provided by China Huaneng Group Co., Ltd.

REFERENCES

Cao, Y., Kurimoto, Y., Zhou, Y. G., et al. (2003). Centrifuge model tests on liquefaction mitigation effect of soil-cement grids under large earthquake loadings. *Bulletin of Earthquake Engineering*, 21(9): 4217-4236. https://doi.org/10.1007/s10518-023-01711-0

Cao, Y., Zhou, Y. G., Ma, Q., et al. (2024). Liquefaction and fluidization responses of level ground retained by sheet-pile wall through centrifuge model tests. *Soil Dynamics and Earthquake Engineering*, 178: 108517. https://doi.org/10.1016/j.soildyn.2024.108517

Ghazy, M. E., Abdoun, T., Dobry, R., et al. (2025) Evaluating the influence of soil stratum thickness on liquefaction potential and overburden correction factor K_σ in silty sand: a centrifuge study. *Journal of Geotechnical and Geoenvironmental Engineering*, 151(9). https://doi.org/10.1061/jggefk.Gteng-13480

Han, J. T., Kim, T. and Cho, W. (2016). Centrifuge modeling of seismic response of normally consolidated deep silt deposit. *Acta Geotechnica*, 11(1): 71-81. https://doi.org/10.1007/s11440-014-0338-8

Ishihara, K. (1993). Liquefaction and flow failure during earthquakes. *Géotechnique*, 43(3): 351-451. https://doi.org/10.1680/geot.1993.43.3.351

Kim, M. K., Lee, S. H., Choo, Y. W., et al. (2011). Seismic behaviors of earth-core and concrete-faced rock-fill dams by dynamic centrifuge tests. *Soil Dynamics and Earthquake Engineering*, 31(11): 1579-1593. https://doi.org/10.1016/j.soildyn.2011.06.010

Kutter, B. L., Carey, T. J., Hashimoto, T., et al. (2018). LEAP-GWU-2015 experiment specifications, results, and comparisons. *Soil Dynamics and Earthquake Engineering*, 113: 616-628. https://doi.org/10.1016/j.soildyn.2017.05.018

Liu, W. J., Wang, S. L., Chen, J. H., et al. (2025) Centrifuge modeling on effectiveness of liquefaction mitigation measures for clayey sand ground under large dams. *Canadian Geotechnical Journal*, 62: 1-14. https://doi.org/10.1139/cgj-2024-0614

Maharjan, M. and Takahashi, A. (2014). Liquefaction-induced deformation of earthen embankments on non-homogeneous soil deposits under sequential ground motions. *Soil Dynamics and Earthquake Engineering*, 66: 113-124. https://doi.org/10.1016/j.soildyn.2014.06.024

Olarte, J., Paramasivam, B., Dashti, S., et al. (2017). Centrifuge modeling of mitigation-soil-foundation-structure interaction on liquefiable ground. *Soil Dynamics and Earthquake Engineering*, 97: 304-323. https://doi.org/10.1016/j.soildyn.2017.03.014

Sharp, M. K. and Adalier, K. (2006) Seismic response of earth dam with varying depth of liquefiable foundation layer. *Soil Dynamics and Earthquake Engineering*, 26(11): 1028-1037. https://doi.org/10.1016/j.soildyn.2006.02.007

Zhou, Y. G., Ma, Q., Liu, K., et al. (2021) Centrifuge model tests at Zhejiang University for LEAP-Asia-2019 and validation of the generalized scaling law. *Soil Dynamics and Earthquake Engineering*, 144: 106660. https://doi.org/10.1016/j.soildyn.2021.106660